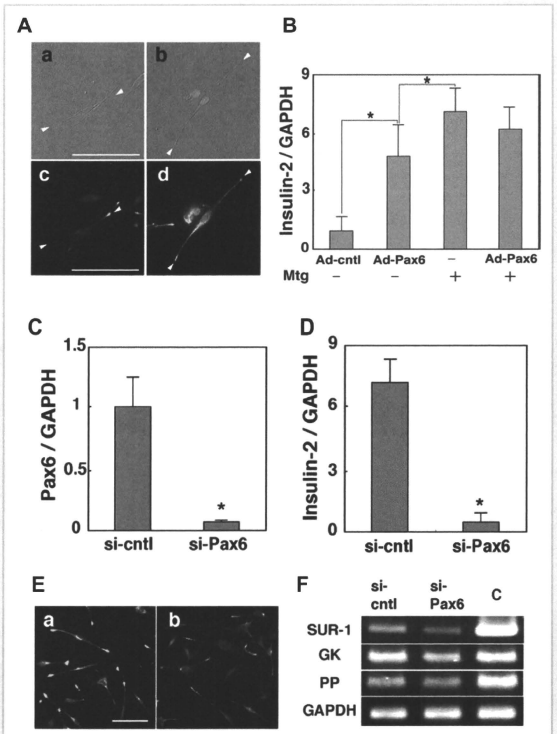

Fig. 3. Effects of overexpression and knockdown of Pax6 on differentiation. A: Morphology of cells overexpressing Pax6. Cells were infected with adenovirus encoding full-length cDNA for mouse Pax6 and incubated for 72 h with 1 nM BTC and 2 nM activin A in BSA-coated dishes. Upper panels (a,b) show morphology of Pax6-transfected cells. Effectively transfected cells were identified by Pax6-specific antibody (red), and the immunostaining of Pax6 was overlaid on Nomarski images (b). Adenovirus encoding lacZ gene was used as control (a). Lower panels (c,d) show overlaid images of Pax6 (red) and insulin (green), which are corresponding images of upper panels. Arrowheads indicated the tip of cell process in a single cell. Bar = 100 μm. B: Effect of overexpression of Pax6 on the expression of mRNA for insulin-2. The expression of mRNA for insulin-2 in Pax6-transfected (Ad-Pax6), LacZ-transfected control (Ad-cntl), non-transfected cells cultured on Matrigel (Mtg) and Pax6-transfected cells cultured on Matrigel was quantified by real-time PCR. Results were normalized to GAPDH. Values are the mean ± SE $^*P < 0.05$. C: Knockdown of pax6 mRNA using siRNA specific to rat Pax6. Cells cultured on matrigel and infected with adenovirus encoding specific siRNA for Pax6 (si-Pax6) and control vectors (si-cntl) were treated with 1 nM BTC and 2 nM activin A. The expression levels of endogenous pax6 mRNA were detected after incubation for 72 h by real-time PCR. Results were normalized to GAPDH and values are the mean ± SE $^*P < 0.05$. D: Effect of knocking down of Pax6 on the expression of mRNA for insulin-2. Cells were treated as in (C), and real-time RCR analysis was performed to quantify the amount of mRNA for insulin-2. Results were normalized to GAPDH and values are the mean ± SE $^*P < 0.05$. E: Effect of siPax on the expression of insulin. Cells transfected with siPax (b) or siLacZ (a) were cultured on Matrigel-coated dishes in the presence of activin A and BTC. Nuclei were stained with DAPI (blue color). Bar = 100 μm. F: Changes in the expression of mRNA for SUR1, glukokinase (GK), and pancreatic polypeptide (PP) in differentiated AR42J cells with or without transfection of si-Pax6.

prepared adenovirus encoding siRNA against Pax6 (Ad-siPax6). Knockdown of Pax6 was significant in Ad-siPax6-transfected cells. The levels of mRNA for Pax6 were reduced to 10% compared to those of the control vector ($P < 0.05$, Fig. 3C). Quantitative RT-PCR analysis showed that silencing of Pax6 significantly reduced the expression of insulin-2 ($P < 0.05$, Fig. 3D). mRNA for insulin-2 in Ad-siPax6-transfected cells was approximately 15% of that of the cells transfected with control vector. Additionally, we found a decrease in insulin immunoreactivities in Ad-siPax6-transfected cells (Fig. 3E). Furthermore, we observed a decrease in mRNA for SUR1 and glucokinase in Ad-siPax6-transfected cells, whereas the expression of mRNA for other hormones including PP, glucagons,

and somatostatin was unchanged (Fig. 3F). Note that we did not observe changes in the expression of other transcription factors (data not shown).

EFFECT OF PURIFIED ECM COMPONENTS ON DIFFERENTIATION

Matrigel contains several basement membrane ECMs including laminin-1, collagen type IV, entactin, fibronectin, and heparin sulfate proteoglycan, and former two are known as major components. To determine which components of the Matrigel regulated differentiation, we examined the effect of laminin-1 and collagen type IV. When the cells were cultured on laminin-1, similar morphological changes as seen in the cells cultured on Matrigel were observed in both undifferentiated (Fig. 4A-c) and differentiated condition (Fig. 4A-g). In addition to morphological changes, we found relatively high levels of mRNA for insulin-2 and Pax6 in differentiated cells cultured on laminin-1 compared to those in cells cultured on plastic dish ($P < 0.05$, Fig. 4B,C) although these effects of laminin-1 were less than those of Matrigel. Furthermore, we also detected relatively high levels and broadly cytoplasmic distributions of insulin immunoreactivities in the cells cultured on laminin-1 (Fig. 4D). On the other hand, obvious morphological changes and upregulation of mRNA for insulin-2 and Pax6 were not observed in the cells cultured on collagen type IV (Fig. 4A-d,A-h,B-D). In addition, we also examined the effect of

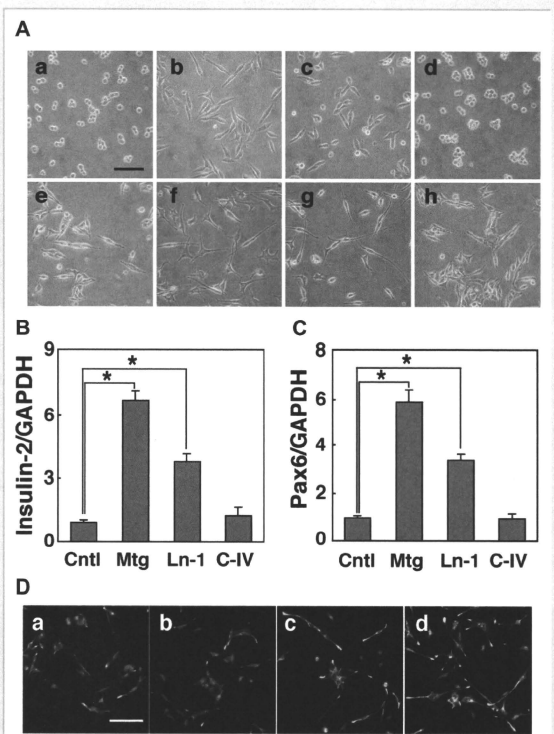

Fig. 4. Effect of purified basement membrane matrix on differentiation. A: Cell morphology. Cells were incubated for 48 h with (e,f,g,h) or without (a,b,c,d) 1 nM BTC and 2 nM activin A on control (a,e), Matrigel-(b,f), laminin-1 (c,g) and collagen type IV (d,h)-coated dishes. Phase-contrast images were presented. Bar = 100 μm. B,C: Quantification of mRNA for insulin-2 and Pax6 in differentiated cells. Cells were incubated for 48 h with 1 nM BTC and 2 nM activin A on control (Cntl), Matrigel (Mtg)-, laminin-1 (Ln-1)- and collagen type IV (C-IV)-coated dishes, and the expression of mRNA for insulin-2 (B) and Pax6 (C) were quantified by real-time PCR. Results are the mean ± SE for three experiments. *$P < 0.05$. D: Insulin-staining of differentiated cells. Cells were cultured as described in (B), and stainings of insulin by immunofluorescence (green) were obtained. A broad cytoplasmic staining pattern of insulin was observed in differentiated cells cultured on Matrigel (d) and laminin-1 (c). a: Control dish. d: Collagen type IV-coated dish. Nuclei were stained with DAPI (blue). Bar = 100 μm.

fibronectin, one of minor component of Matrigel but no obvious changes were observed (data not shown). These data suggest that laminin-1 is the major component of Matrigel responsible for its positive effects on differentiation in AR42J cells although involvement of other signaling molecules in Matrigel is not excluded.

INHIBITORY EFFECT OF ANTI *B*-1 INTEGRIN ANTIBODY ON DIFFERENTIATION

To investigate the molecules that integrate the signals from ECM, we focused on the role of β1-integrin since it is a common integrin receptor isoform corresponding to laminins and is believed to be important for islet cell development [Jiang et al., 2002; Wang et al., 2005; Kren et al., 2007; Yashpal et al., 2008]. As shown in Figure 5A, we found that the expression of β1-integrin was detected in naive cells. Interestingly, the expression of β1-integrin was markedly increased in differentiated cells. The increases in β1-integrin expression in differentiated cells were observed in those cultured on Matrigel, and the expression levels between these cells were not different (data not shown). We then analyzed the effect of anti-β1-integrin antibody on the morphology of the cells cultured on Matrigel. In non-differentiated condition, anti-β1 integrin antibody inhibited morphological changes induced by Matrigel, and cells remained round-shaped (Fig. 5B-b). Cells treated with control antibody were not affected (Fig. 5B-a). In a differentiated condition, cells incubated with anti-β1-integrin antibody were less spread out with shorter processes (Fig. 5B-e,B-f). In contrast, cells cultured on control dish were not affected by anti-β1-integrin antibody in either non-differentiated and differentiated conditions (Fig. 5B-c,B-d,B-g,B-h). These inhibitory effects of anti-β1 integrin antibody were also observed in the cells cultured on laminin-1 (data not shown). By quantitative RT-PCR analysis, we also found a significant reduction of the expression of mRNA for insulin-2 and Pax6 in differentiated cells cultured on Matrigel and laminin-1 with anti-β1-integrin antibody (Fig. 5C,D). Conversely, no remarkable changes in insulin and Pax6 were observed in differentiated cells incubated with anti-β1-integrin antibody when the cells were cultured on control dish. Furthermore, we also confirmed decrease in the insulin signal in differentiated cells cultured on Matrigel treated with anti-β1-integrin (Fig. 5E-a,

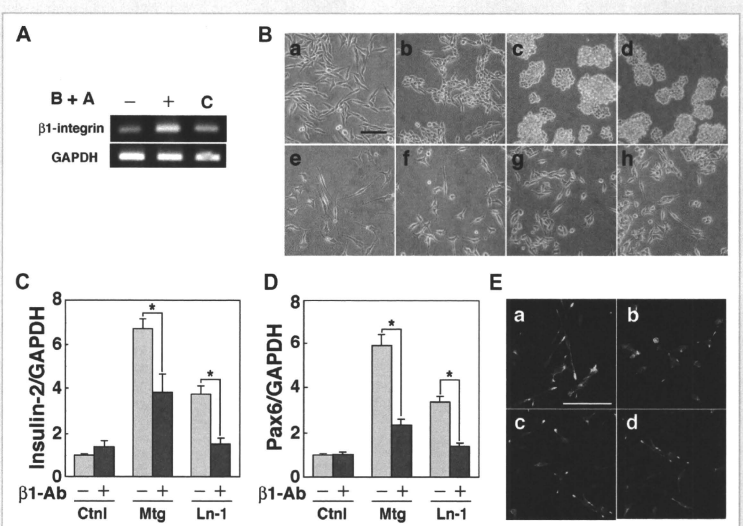

Fig. 5. Effect of anti-β1 integrin antibody on morphological appearance and endocrine differentiation on matrigel and laminin-1. A: Changes in the Expression of mRNA for β1 Integrin. Cells were incubated for 48 h with (+) or without (–) activin A and betacellulin (B + A) on BSA-coated dishes. mRNA for β1 integrin was measured by RT-PCR and mRNA from INS-1 was used as a control (C). B: Effect of Anti-β1 integrin antibody on morphology. Cells cultured on Matrigel (a,b,e,f) or BSA-coated (c,d,g,h) dishes were treated with anti-β1 integrin antibody (b,f,d,h) or control IgM (a,c,e,g). Phase contrast images were obtained 12 h after treatment with (e–h) or without (a–d) activin A and BTC. Bar = 100 μm. C,D: Quantification of mRNA for insulin-2 and Pax6. Cells cultured on Matrigel- (Mtg) and laminin-1 (Ln-1)-coated dishes were incubated for 48 h with activin A and BTC in the presence (+) or absence (–) of anti-β1 integrin antibody (β1-Ab). mRNA for insulin-2 (C) or Pax6 (D) was quantified by real-time PCR. Results were normalized to GAPDH and values are the mean ± SE of three independent experiments. *$P < 0.05$. E: Immunofluorescence staining of insulin in differentiated cells. Cells were cultured on Matrigel- (a,b) or BSA-coated (c,d) (control) dishes in the presence of anti-β1 integrin antibody (b,d) or control IgM (a,c). They were then incubated with activin A and BTC for 48 h. Immunoreactive insulin is shown in green. Nuclei were stained with DAPI (blue). Bar = 100 μm.

E-b), whereas no remarkable change in insulin signal was observed in those cultured on plastic dish (Fig. 5E-c,E-d). The reduction of insulin signals were also observed in anti-β1 integrin antibody treated cells cultured on laminin-1 (data not shown). These results suggest that β1-integrins are involved in the stimulatory effect of Matrigel and laminin-1 on differentiation.

EFFECT OF BASEMENT MEMBRANE INVOLVES p38 MAP KINASE

Our previous studies demonstrated the involvement of p42/44MAPK and p38MAPK but not PI-3kinase and JNK in endocrine differentiation of AR42J cells [Furukawa et al., 1999; Kitamura et al., 2007]. Integrin exerts its cellular responses by regulating these intracellular signaling molecules [Mainiero et al., 2000; Bhowmic et al., 2001]. We therefore studied the effects of Matrigel on the phosphorylation of p38 and p42/44 MAP kinases during differentiation. As shown in Figure 6A, a relatively high amount of phosphorylated p38 was observed in cells cultured on Matrigel. In contrast, no remarkable differences in the amount of phosphorylated p42/44 MAP kinase were observed. Similar patterns of phosphorylations of p38 and p42/44 were also observed in the cells cultured on laminin-1 (data not shown). Additionally, when the cells were incubated with anti-β1 antibody, the increase in the amount of phosphorylated p38 MAP kinase induced by Matrigel was reduced (Fig. 6B). Also, addition of SB203580 attenuated Matrigel-induced activation of p38 MAP kinase (Fig. 6C) and completely blocked the expression of insulin.

EFFECT OF ECMS ON DIFFERENTIATION OF PANCREATIC DUCTAL CELLS

Finally, we addressed whether basement membrane affects differentiation of pancreatic ductal cells to insulin-producing cells in vitro. Ductal cells were cultured on Matrigel and treated with activin and BTC. Cells were incubated for 7 days and insulin content was measured. As depicted in Figure 7A, the expression of mRNA for insulin in cells cultured in Matrigel-coated dishes was markedly higher than those cultured on control dish. Similarly, the insulin content was increased in cells cultured on Matrigel-coated dishes (Fig. 7B). As shown in Figure 7C, the expression of Pax6 was upregulated in cells cultured on Matrigel-coated dishes. The increase in the insulin content was inhibited by anti-β1-integrin antibody (data not shown).

DISCUSSION

We showed that appropriate culture system promoted β-cell differentiation in both pancreatic progenitor-like cell lines and

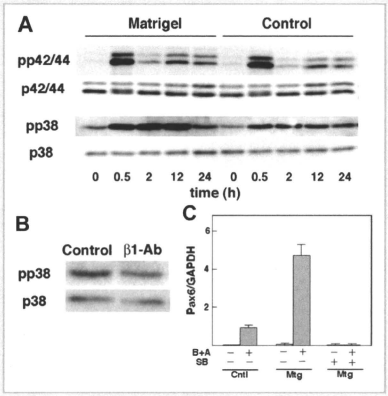

Fig. 6. Effect of matrigel on the activation of mitogen-activated kinases. A: Analysis of phosphorylation of p42/44 MAPK and p38 MAPK during differentiation. Cells cultured on matrigel or BSA (Control) were incubated for indicated time with a combination of activin A and BTC, and phosphorylation of p42/44 and p38 MAP kinases was analyzed by immnoblotting. B: Effect of anti-β1 integrin antibody on phosphorylation of p38 MAPK. Cells were preincubated with or without anti-β1 integrin antibody (β1 Ab) for 15 min and cultured on Matrigel in the presence of BTC and activin A. The cells were harvested 2 h after the treatment with BTC and activin A and Western blot analysis for p38 was performed. Typical images among the three independent analyses are shown. C: Effect of SB203580 on the expression of Pax6. Cells cultured on BSA-coated (Cntl) or Matrigel-coated (Mtrg) dishes were stimulated by activin A and BTC in the presence and absence of 10 μM SB203580 and the expression of Pax6 was measured by quantitative PCR.

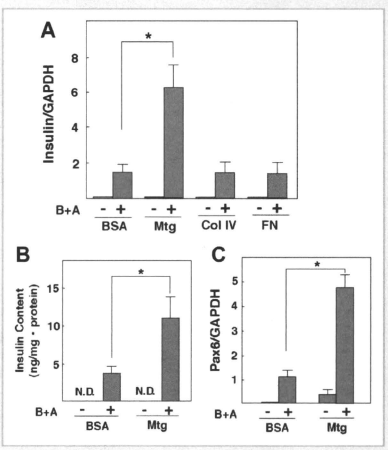

Fig. 7. Effect of ECM on differentiation of ductal cells. A: Expression of mRNA for insulin. Ductal cells were incubated for 7 days with 1 nM BTC and 2 nM activin A (B + A) in control-, Matrigel- (Mtg), collagen type IV- (col IV) and fibronectin-coated (FN) dishes. The expression of insulin was analyzed by real-time PCR. Results are shown as the mean ± SD for four experiments; $^*P < 0.05$. B: Changes in the insulin content. Ductal cells were incubated as indicated above and the insulin content was measured. Results are the mean ± SD for four experiments; $^*P < 0.05$. C: Changes in the expression of Pax6. Ductal cells were incubated with activin A and BTC for 48 h and the expression of Pax6 was measured by real-time PCR. Results are shown as the mean ± SD for four experiments; $^*P < 0.05$.

cultured duct epithelial cells. We found that Matrigel exerted the effect on β-cell differentiation through induction of Pax6, and the effect was reproduced at least partly by an individual ECM component, laminin-1. Additionally, using the blocking antibody we demonstrated that these favorable effects of basement membrane on β-cell differentiation were exerted through the interaction with β-1 integrin. Our data suggest that the basement membrane plays a crucial role in the regulation of β-cell differentiation and appropriate expression of transcriptional factors.

Several studies suggested the importance of the basement membrane in β-cell development [Lammert et al., 2001; Yoshitomi and Zaret, 2004]. In addition, the effectiveness of Matrigel in adult pancreatic duct cells and fetal pancreatic cells is reported [Jiang et al., 1999; Bonner-Weir et al., 2000]. These approaches using pancreatic explant may reflect physiological conditions, but it is unfavorable to study the molecular signalings due to heterogeneous cell population. In the present study, we used a simple model cell line reproducing β-cell differentiation. In agreement with previous studies, we demonstrated that reconstitute basement membrane, Matrigel was an effective substrate for differentiation in AR42J cells. Matrigel induced morphological changes and enhancement of the insulin expression during differentiation. Interestingly, we found the morphological changes comparable to those observed in activin-treated cells even in Matrigel-exposed cells without differentiation factors. Although Matrigel-exposed cells did not convert to endocrine cells expressing insulin or PP, these cells showed decrease in amylase expression in parallel with the increase in cytokeratin-20, a marker of pancreatic ductal cells (data not shown). Thus, Matrigel by itself may act on the initial step of differentiation although signals of differentiation factors are still required to convert to endocrine cells. This notion is supported by the concept that pancreatic progenitor cells in vivo are derived from ductal epithelium [Bonner-Weir and Weir, 2005]. In addition to enhancement of the insulin expression, Matrigel-exposed cells express more mature functions. This was evident by the following findings: upregulation of the expression of β-cell markers including SUR1, glucokinase and Pax6 [Sander et al., 1997; St-Onge et al., 1997; Ashery-Padan et al., 2001]; and intense and broadly cytoplasmic accumulation of insulin immunoreactivities. These results strongly suggest that the basement membrane component promotes differentiation. Our findings obtained in AR42J cells are advantageous in several respects compared to those of the previous data obtained in vivo and in vitro. In particular, since AR42J is a clonal cell line, they provide a good experimental system to study the regulation of differentiation and to identity the genes involved [Mashima et al., 1999; Kren et al., 2007]. Indeed, using this model system, we demonstrated the contribution of Pax6 (see below). Note that AR42J is slightly different from progenitors observed in vivo. For example, differentiated AR42J cells express low amount of insulin and lack some transcription factors including islet-1, Nkx6.1 and Maf A. Nonetheless, because we observed similar responsiveness to the basement membrane in ductal cells, AR42J is a useful model for investigating cellular signaling during β-cell differentiation.

Using this cell model, we addressed the intracellular signaling molecules involved in the basement membrane-induced enhancement of differentiation, in particular, the contribution of transcription factors. Of various transcription factors investigated, upregulation of Pax6 was demonstrated. This was observed only when cells were treated with differentiation factors and Matrigel, suggesting that cooperative signalings from extracellular matrix and growth factors are required for its expression. Interestingly, severe reduction of Pax6 expression in Xenopus embryonic endoderm is observed when the embryo is dissociated from the basement membrane of dorsal aorta [Lammert et al., 2001]. These findings strongly indicate that signals from the basement membrane are required for appropriate expression of transcription factor. We demonstrated the role of Pax6 in two ways: by a gain of function study and by a knockdown study. The gain of function study of Pax6 demonstrated up-regulation of insulin both in mRNA and protein levels. Overexpression of Pax6 also induced morphological changes comparable to these observed in Matrigel-exposed cells. However, Pax6-overexpressing cells also produced other hormones including glucagon and somatostatin. These findings indicate that induction of Pax6 reproduces differentiation-inducing activity of Matrigel, but the effect was not completely the same. The induction of glucagon and somatostatin in Pax6-overexpressing cells is not surprising since Pax6 also regulates transcription of these hormones as well as insulin [Sander et al., 1997; Cissell et al., 2003]. Unphysiologically excessive amounts of Pax6 may affect transcriptional regulation of these hormones. Consistent with this notion, we found a marked reduction of Pax4 and Nkx2.2 in Pax6-overexpressing cells (data not shown). Additionally, transgenic mice overexpressing Pax6 in islets exhibit glucagon and insulin double-positive cells and disruption of normal islet structures in the pancreas [Yamaoka et al., 2000]. In contrast to the results of the gain of function experiment, knockdown of Pax6 clearly attenuated upregulation of insulin and other β-cell markers. These effects were due to specific reduction of Pax6 since the expressions of other transcriptional factors were not changed. Taken together, Pax6 plays a key role in Matrigel-mediated differentiation in this model system. Pax6 is known to have a pleiotropic role in the development of the endocrine pancreas, and it is also thought to play an important role in α-, β-, δ-, and PP-cells [Sander et al., 1997; St-Onge et al., 1997]. With regard to the β-cell functions, Pax6 directly and indirectly regulates the expression of mature β-cell markers such as insulin, GLUT2, glucokinase, and IAPP [Sander et al., 1997; Ashery-Padan et al., 2001; Cissell et al., 2003]. However, Pax6 knockout mice do not show complete loss of β-cells [Sander et al., 1997; Murtaugh, 2006]. It is therefore considered to regulate maturation of β-cells rather than determination of the cell fate. The results of the present study are consistent with those aspects of Pax6. Indeed, AR42J cells could differentiate into insulin-producing cells independent of the presence of Pax6 [Zhang et al., 2001]. Collectively, the functions of Pax6 in basement membrane-mediated differentiation may be mainly due to promotion of maturation rather than determination of the cell fate. It is unclear which signals induce the expression of Pax6 and how Pax6 promotes β-cell differentiation.

We have also found that integrin-activated signal transduction pathways are responsible for the regulation of differentiation induced the by the basement membrane. Specific antibody against

β1-intengrin abrogated upregulation of insulin and Pax6 induced by Matrigel and laminin-1. Particularly, the effect of laminin-1 is almost completely abolished by the treatment with blocking antibody. Note that anti-β1 integrin blocking antibody did not affect differentiation in cells cultured on control dish. This indicates that differentiation of AR42J cells itself occurred independently of β1-integrin signaling. Alternatively, it also possible that AR 42J cells do not produce effective ECMs binding to β1 integrin enough to promote differentiation. Consistent with this hypothesis, we confirmed only low levels of laminin expression in AR42J cells (data not shown). These lines of evidence support the importance of exogenous supplementation of basement membrane for appropriate β-cell differentiation in vitro. Our data agree with the previous study showing that reduction of insulin expression in neonatal islet cells in which β1-integrin interaction is abrogated by gene silencing and the treatment with the blocking antibody [Yashpal et al., 2008]. Our results also extend by showing the role of β1 integrin in regulating the expression of transcription factors.

We also demonstrated the involvement of p38 during differentiation. We found relatively high amounts of phosphorylated p38 in cells cultured on Matrigel and they were abrogated by blocking antibody against β1-integrin (Fig. 6A,B). This indicates that p38 is in downstream of the β1-integrin signaling. These crosstalks of growth factor and β1-integrin signaling in modulating stress kinases are demonstrated by several studies [Mainiero et al., 2000; Bhowmic et al., 2001]. Given that overexpression of transforming growth factor-β-activated kinase 1, an upstream regulator of p38, promotes endocrine differentiation [Ogihara et al., 2003], we postulate that p38 activation is involved in basement membrane-induced differentiation. Interestingly, activation of p38 enhances transcriptional activities of Pax6 through the phosphorylation of its transactivation domain [Mikkola et al., 1999]. Also, β1-integrin-dependent induction of Pax6 during lens development is demonstrated in mice with lens-specific ablation of β1-integrin [Simirskii et al., 2007]. These molecules may modify the function of Pax6, which contributes to promotion of β-cell differentiation induced by the basement membrane. Further studies are needed to clarify the downstream signals of integrin receptor that control regulatory network of the transcriptional factors.

Our findings provide a new insight into the understanding of the role of ECMs in β-cell differentiation. Several lines of evidence indicate that signals from ECM contribute to improved β-cell functions including insulin secretion, glucose responsiveness, and survival [Wang et al., 2005; Parnaud et al., 2006; Pinkse et al., 2006]. However, most of these studies focus on the contribution of ECM to the maintenance of cell functions in isolated β-cells. Our data demonstrate an additional role of the basement membrane as a modulator of β-cell differentiation, and Pax6 is involved in this action. These findings may be helpful to establish cell replacement therapy for diabetes using precursor cells. For instance, when the pancreatic precursor cells are used for the source of β-cell transplantation, the use of basement membrane may promote differentiation to β-cells. Our approach using natural agents is safer than virus-based methods which are well-used to obtain insulin-producing cells. Positive roles of ECMs in β-cell differentiation have been reported in ES cells [Schroeder et al., 2006].

In summary, basement membrane promoted differentiation of AR42J and ductal cells into insulin-producing cells. This effect may be exerted through upregulation of Pax6. These findings provide a new insight into our understanding of the mechanisms for ECM-mediated β-cell differentiation.

REFERENCES

Ahlgren U, Pfaff SL, Jessell TM, Edlund T, Edlund H. 1997. Independent requirement for ISL1 in formation of pancreatic mesenchyme and islet cells. Nature 385:257–260.

Artner I, Blanchi B, Raum JC, Guo M, Kaneko T, Cordes S, Sieweke M, Stein R. 2007. MafB is required for islet beta cell maturation. Proc Natl Acad Sci USA 104:3853–3858.

Ashery-Padan R, Zhou T, Marquardt X, Herrera P, Toube L, Berry A, Gruss P. 2001. Conditional inactivation of Pax6 in the pancreas causes early onset of diabetes. Dev Biol 269:479–488.

Bhowmic NA, Zent R, Ghiassi M, McDonnell M, Moses HL. 2001. Integrin beta 1 signaling is necessary for transforming growth factor-beta activation of p38MAPK and epithelial plasticity. J Biol Chem 276:46707–46713.

Bonner-Weir S, Weir GC. 2005. New sources of pancreatic beta-cells. Nat Biotechnol 23:857–861.

Bonner-Weir S, Taneja M, Weir GC, Tatarkiewicz K, Song KH, Sharma A, O'Neil JJ. 2000. In vitro cultivation of human islets from expanded ductal tissue. Proc Natl Acad Sci USA 97:7999–8004.

Cissell MA, Zhao L, Sussel L, Henderson E, Stein R. 2003. Transcription factor occupancy of the insulin gene in vivo. Evidence for direct regulation by Nkx2.2. J Biol Chem 278:751–756.

Furukawa M, Zhang YQ, Nie L, Shibata H, Kojima I. 1999. Role of mitogen-activated protein kinase and phosphoinositide 3-kinase in the differentiation of rat pancreatic AR42J cells induced by hepatocyte growth factor. Diabetologia 42:450–456.

Harrison KA, Thaler J, Pfaff SL, Gu H, Kehrl JH. 1995. Pancreas dorsal lobe agenesis and abnormal islets of Langerhans in Hlxb9-deficient mice. Nat Genet 23:71–75.

Hynes RO. 2002. Integrins: Bidirectional, allosteric signaling machines. Cell 110:673–687.

Jiang FX, Cram DS, DeAizpurua HL, Harrison LC. 1999. Laminin-1 promotes differentiation of fetal mouse pancreatic beta-cells. Diabetes 48:722–730.

Jiang FX, Naselli G, Harrison LC. 2002. Distinct distribution of laminin and its integrin receptors in the pancreas. J Histochem Cytochem 50:1625–1632.

Jonsson J, Carlsson L, Edlund T, Edlund H. 1994. Insulin-promoter-factor 1 is required for pancreas development in mice. Nature 371:606–609.

Kitamura R, Ogata T, Tanaka Y, Motoyoshi K, Seno M, Takei I, Umezawa K, Kojima I. 2007. Conophylline and betacellulin-delta4: An effective combination of differentiation factors for pancreatic beta cells. Endocr J 54:255–264.

Kren A, Baeriswyl V, Lehembre F, Wunderlin C, Strittmatter K, Antoniadis H, Fässler R, Cavallaro U, Christofori G. 2007. Increased tumor cell dissemination and cellular senescence in the absence of beta1-integrin function. EMBO J 26:2832–2842.

Lammert E, Cleaver O, Melton D. 2001. Induction of pancreatic differentiation by signals from blood vessels. Science 294:564–567.

Li H, Arber S, Jessell TM, Edlund H. 1999. Selective agenesis of the dorsal pancreas in mice lacking homeobox gene Hlxb9. Nat Genet 23:67–70.

Mainiero F, Soriani A, Strippoli R, Jacobelli J, Gismondi A, Piccoli M, Frati L, Santoni A. 2000. RAC1/P38 MAPK signa ling pathway controls beta1 integrin-induced interleukin-8 production in human natural killer cells. Immunity 12:7–16.

Mashima H, Ohnishi H, Wakabayashi K, Mine T, Miyagawa J, Hanafusa T, Seno M, Yamada H, Kojima I. 1996. Betacellulin and activin A coordinately convert amylase-secreting pancreatic AR42J cells into insulin-secreting cells. J Clin Invest 97:1647–1654.

Mashima H, Yamada S, Tajima T, Seno M, Yamada H, Takeda J, Kojima I. 1999. Genes expressed during differentiation of pancreatic AR42J cells to insulin-secreting cells. Diabetes 48:304–309.

Mikkola I, Bruun JA, Bjorkoy G, Holm T, Johansen T. 1999. Phosphorylation of the transactivation domain of Pax6 by extracellular signal-regulated kinase and p38 mitogen-activated protein kinase. J Biol Chem 274: 15115–15126.

Murtaugh LC. 2006. Pancreas and beta-cell development: From the actual to the possible. Development 134:427–438.

Naya FJ, Huang HP, Qiu Y, Mutoh H, DeMay AB, Leiter Tsai MJ. 1997. Diabetes, defective pancreatic morphogenesis, and abnormal enteroendocrine differentiation in BETA2/neuroD-deficient mice. Genes Dev 11:2323–2334.

Nikolova G, Jabs N, Konstantinova I, Domogatskaya A, Tryggvason K, Sorokin L, Fässler R, Gu G, Gerber HP, Ferrara N, Melton DA, Lammert E. . The vascular basement membrane: A niche for insulin gene expression and Beta cell proliferation. Dev Cell 10:397–405.

Offield MF, Jetton TL, Labosky PA, Ray M, Stein RW, Magnuson MA, Hogan BL, Wright CV. 1996. PDX-1 is required for pancreatic outgrowth and differentiation of the rostral duodenum. Development 122:983–995.

Ogata T, Li K, Seno M, Kojima I. 2004. Reversal of streptozotocin-induced diabetes by transplantation of β cells derived from ductal cells. Endocr J 51:381–386.

Ogihara T, Watada H, Kanno R, Ikeda F, Nomiyama T, Tanaka Y, Nakao A, German MS, Kojima I, Kawamori R. 2003. p38 MAPK is involved in activin A- and hepatocyte growth factor-mediated expression of pro-endocrine gene neurogenin 3 in AR42J-B13 cells. J Biol Chem 278:21693–21700.

Ohnishi H, Ohgushi N, Tanaka S, Mogami H, Nobusawa R, Mashima H, Furukawa M, Mine T, Shimada O, Ishikawa H, Kojima I. 1995. Conversion of amylase-secreting rat pancreatic AR42J cells to neuronlike cells by activin. J Clin Invest 95:2304–2314.

Olbrot M, Rud J, Moss LG, Sharma A. 2002. Identification of beta-cell-specific insulin gene transcription factor RIPE3b1 as mammalian MafA. Proc Natl Acad Sci USA 99:6737–6742.

Parnaud G, Hammar E, Rouiller DG, Armanet M, Halban PA, Bosco D. 2006. Blockade of beta1 integrin-laminin-5 interaction affects spreading and insulin secretion of rat beta-cells attached on extracellular matrix. Diabetes 55:1413–1420.

Pinkse GG, Bouwman WP, Jiawan-Lalai R, Terpstra OT, Bruijn JA, de Heer E. 2006. Integrin signaling via RGD peptides and anti-beta1 antibodies confers resistance to apoptosis in islets of Langerhans. Diabetes 55:312–317.

Riquelme C, Larrain J, Schonherr E, Henriquez JP, Kresse H, Brandan E. 2001. Antisense inhibition of decorin expression in myoblasts decreases cell responsiveness to transforming growth factor beta and accelerates skeletal muscle differentiation. J Biol Chem 276:3589–3596.

Sander M, Neubüser A, Kalamaras J, Ee HC, Martin GR, German MS. 1997. Genetic analysis reveals that PAX6 is required for normal transcription of pancreatic hormone genes and islet development. Genes Dev 11:1662–1673.

Sander M, Sussel L, Conners J, Scheel D, Kalamaras J, Dela Cruz F, Schwitzgebel V, Hayes-Jordan A, German M. 2000. Homeobox gene Nkx6.1 lies downstream of Nkx2.2 in the major pathway of beta-cell formation in the pancreas. Development 127:5533–5540.

Schroeder IS, Rolletschek A, Blyszczuk P, Kania G, Wobus AM. 2006. Differentiation of mouse embryonic stem cells to insulin-producing cells. Nat Protoc 1:495–507.

Seno M, Tada H, Kosaka M, Sasada R, Igarashi K, Shing Y, Folkman J, Ueda M, Yamada H. 1996. Human betacellulin, a member of the EGF family dominantly expressed in pancreas and small intestine, is fully active in a monomeric form. Growth Factors 13:181–191.

Simirskii VN, Wang Y, Duncan MK. 2007. Conditional deletion of beta1-integrin from the developing lens leads to loss of the lens epithelial phenotype. Dev Biol 306:658–668.

Sosa-Pineda B, Chowdhury K, Torres M, Oliver G, Gruss P. 1997. The Pax4 gene is essential for differentiation of insulin-producing beta cells in the mammalian pancreas. Nature 386:399–402.

St-Onge L, Sosa-Pineda B, Chowdhury K, Mansouri A, Gruss P. 1997. Pax6 is required for differentiation of glucagon-producing alpha-cells in mouse pancreas. Nature 387:406–409.

Sussel L, Kalamaras L, Hartigan-O'Connor DL, Meneses JJ, Pedersen RA, Rubenstein JL, German MS. 1998. Mice lacking the homeodomain transcription factor Nkx2.2 have diabetes due to arrested differentiation of pancreatic beta cells. Development 125:2213–2221.

Suzuki A, Iwama A, Miyashita H, Nakauchi H, Taniguchi H. 2003. Role for growth factors and extracellular matrix in controlling differentiation of prospectively isolated hepatic stem cells. Development 130:2513–2524.

Wang R, Li J, Lyte K, Yashpal NK, Fellows F, Goodyer CG. 2005. Role for beta1 integrin and its associated alpha3, alpha5, and alpha6 subunits in development of the human fetal pancreas. Diabetes 54:2080–2089.

Yamaoka T, Yano M, Yamada T, Matsushita T, Moritani M, Ii S, Yoshimoto K, Hata J, Itakura M. 2000. Diabetes and pancreatic tumours in transgenic mice expressing Pax 6. Diabetologia 43:332–339.

Yashpal NK, Li J, Wheeler MB, Wang R. 2008. Expression of {beta}1 integrin receptors during rat pancreas development–Sites and dynamics. Endocrinology 146:1798–1807.

Yoshitomi H, Zaret KS. 2004. Endothelial cell interactions initiate dorsal pancreas development by selectively inducing the transcription factor Ptf1a. Development 131:807–817.

Zhang YQ, Mashima H, Kojima I. 2001. Changes in the expression of transcription factors in pancreatic AR42J cells during differentiation into insulin-producing cells. Diabetes 50 (Suppl 1):S10–S14.

African Journal of Biotechnology Vol. 10(3), pp. 449-452, 17 January, 2011
Available online at http://www.academicjournals.org/AJB
ISSN 1684–5315 © 2011 Academic Journals

Full Length Research Paper

Construction of a high-efficiency multi-site-directed mutagenesis

Haidong Tan[1], Yueguang Li[2], Ling Chen[3], Tomonari Kasai[3] and Masaharu Seno[3]*

[1]Biotechnology Department, Dalian Institute of Chemical Physics, Chinese Academy of Sciences, 457 Zhongshan Road, Dalian 116023, People's Republic of China.
[2]Department of General Surgery, Tianjin 4th Centre Hospital, Zhongshanlu, Hebeiqu, Tianjin 300140, People's Republic of China.
[3]Department of Medical and Bioengineering Science, Graduate School of Natural Science and Technology, Okayama University, Okayama 700-8530, Japan.

Accepted 15 November, 2010

Although site-directed mutagenesis has been used in many fields, it still has low rate of success and high cost because of low-yield target products. A modified method for multi-site-directed mutagenesis was developed with shifted primer design and cold-start polymerase chain reaction (PCR). The developed method was successfully applied to hexapeptide gene synthesis and recombinant enterokinase gene modification in the plasmids pET41a and pET24b-EK. The efficiency was pronounced at a 1:10 molar ratio of 7-base mutant products to 705-bp fragment products as control. Even in a 10-base substitution mutagenic PCR, a 1:50 molar ratio of mutant products to 705-bp fragment products was reached. Meanwhile, the quality of mutants was proved through the transformation efficiency and sequencing. This method was beneficial to prepare high-quality multibase mutagenesis and also implied that large-scale multibase mutagenesis was feasible, efficient, economical, and productive.

Key words: Site-directed multibase mutagenesis, shift primer, hexapeptide gene, enterokinase gene.

INTRODUCTION

Multi-site-directed mutagenesis (MSD) is a powerful tool to modify DNA sequences in molecular biological studies (Mullaney et al., 2010; Shaya et al., 2010; Zhao et al., 2010). The simplest and most broadly applicable protocol is the quick-change site-directed mutagenesis system developed by Stratagene Company. With this approach, the mutation is introduced in a single polymerase chain reaction (PCR) with one pair of complementary primer containing the interesting mutation. In this method, primer dimer will be easily formed rather than the primer-template annealing. Thus, mutational studies will become more difficult because it often fail to introduce any mutation. Later, the problem was overcome by Zheng et al. (2004). However, we still confronted many difficulties even when using the optimal method. This led us to explore more methods to improve the PCR and make MSD available.

Recombinant hexapeptide (Falla and Zhang, 2010) and enterokinase (EK) were two products developed in our laboratory. The gene for the hexapeptide could be synthesized easily in the plasmid pET41a through MSD since it is coded by an 18-base gene. The latter was expressed as inclusion body in BL21 (DE3) with no bioactivity after refolding, which was caused by its wrong sequences; therefore MSD could be used to amplify the gene or correct wrong sequences directly. Meanwhile, the rules for PCR-based MSD were exploited. The work was directed toward better definition of basic processes and the development of analytical procedures that could be

*Corresponding author. E-mail: mseno@cc.okayama-u.ac.jp. Fax: +81-86-251-8216.

Abbreviations: PCR, Polymerase chain reaction; **MSD,** multi-site-directed mutagenesis; **EK,** enterokinase; **LB,** lysogenic broth; **ccc,** circular covalently closed.

Table 1. The primer pair comparison between QuickChange-site-directed mutagenesis system and our study.

Primer sequence	Length/ mutation (bases)	Successive complementarity of primer pair (bases)	Self-annealing Tm (˚C)
HP_f** 5'-CGACGACAAGgaagagatgcaacgtcgctAGTCCCATGGGA-3'	41/19	39	70.8
HP_r** 5'-CCATGGGACTagcgacgttgcatctcttcCTTGTCGTCGTCA-3'	42/19		
HP_f* 5'-ACAAGgaagagatgcaacgtcgctAGTCCCATGGGA-3'	36/19	29	62.9
HP_r* 5'-GGACTagcgacgttgcatctcttcCTTGTCGTCGTCA-3'	37/19		
HP_f 5'-gaagagatgcaacgtcgctAGTCCCATGGGATATC-3'	35/19	19	51.1
HP_r 5'-agcgacgttgcatctcttcCTTGTCGTCGTCATCAC-3'	36/19		
HP1_f** 5'-CGACGACAAGgaagagATGGGATATCGGGGATC-3'	33/6	26	59.5
HP1_r** 5'-GATATCCCATctcttcCTTGTCGTCGTCATCACC-3'	34/6		
HP1_f* 5'-ACAAGgaagagATGGGATATCGGGGATC-3'	28/6	21	43.4
HP1_r* 5'-CCCATctcttcCTTGTCGTCGTCATCACC-3'	29/6		
HP1_f 5'-gaagagATGGGATATCGGGGATC-3'	23/6	6	18
HP1_r 5'-ctcttcCTTGTCGTCGTCATCACC-3'	24/6		
HP2_f** 5'-GGAAGAGATGcaacgtcgctGATCCGAATTCTGTACAG-3'	38/10	31	64.4
HP2_r** 5'-GAATTCGGATCagcgacgttgCATCTCTTCCTTGTCGTC-3'	39/10		
HP2_f* 5'-AGATGcaacgtcgctGATCCGAATTCTGTACAG-3'	33/10	26	53.8
HP2_r* 5'-GGATCagcgacgttgCATCTCTTCCTTGTCGTC-3'	33/10		
HP2_f 5'-caacgtcgctAGTCCCATGGGATATC-3'	27/10	10	32
HP2_r 5'-agcgacgttgCTTGTCGTCGTCATC-3'	27/10		
EK1_f** 5'-GATATACATATGgTTGTCGGAGGAAGTGACTC-3'	32/7	26	56.4
EK1_r** 5'-CTTCCTCCGACAAcCATATGTATATCTCCTTC-3	32/7		
EK1_f* 5'-ATATGgTTGTCGGAGGAAGTGACTC-3'	23/7	5	30
EK1_r* 5'-GACAAcCATATGTATATCTCCTTC-3'	21/7		

For all primers, mutagenized positions are denoted in lowercase. The single asterisk stands for the primer with the mutation site at the fifth base from the 5'-terminus. The primers without asterisk have the mutation site at the 5'-terminus. The primers, which are designed according to the instructions given by Strategene Company, are marked with double asterisk. In all the primers of EK, there is a 6-base deletion compared with partial template: 5'-CATATG~~GCTAGC~~ATTGTCGGAGGAAG-3'.

applied to successful mutagenesis.

MATERIALS AND METHODS

Plasmid construction

Plasmids pET41a and pET24b-EK were used as mutagenic templates. All primers designed to introduce multibase mutations were synthesized and purified by Takara and all restriction enzymes were purchased from Takara (Dalian, China). *Pfu* DNA polymerase and competent cells were purchased from Dingguo Biotech (Beijing, China), while *Dpn* I was purchased from Biolabs (Beijing, China). The self-annealing temperature (Tm) of the primer was calculated with the formula given by Stratagene (http://www.stratagene.com/manuals/200519.pdf). The characteristics of the primers are listed in Table 1. The gene fragment 5'-GAAGAGATGCAACGTCGC-3' encoding hexapeptide EEMQRR was inserted into the downstream of the EK cleaving site. EK gene (AY682203) was cloned into pET-24b at the *Nde* I/*Xho* I sites.

PCR mutagenesis

One hundred ng (1 µl) plasmid pET41a or pET24b-EK was used as mutagenesis template. Five µl *Pfu* DNA polymerase buffer 10× reaction buffer, 2 µl primers (each at a concentration of 20 µM), 2 µl (4 U) *Pfu* DNA polymerase, 2 µl dNTP mix (10 mM each) and 36 µl water were combined and placed in the block of a Eppendorf temperature cycler, at 95°C for 2 min, followed by 18 cycles of 95°C for 1 min, 55°C for 1.5 min, and 68°C for 14 min. Finally, one cycle of 68°C was carried out for 14 min.

Another PCR was performed with cold start. 100 ng (1 µl) plasmid pET41a or pET24b-EK was used as mutagenesis template. Five µl *Pfu* DNA polymerase buffer 10 × reaction buffer, 2 µl primers (each at a concentration of 20 µM), and 36 µl water were combined and placed in the block of an Eppendorf temperature cycler, at 95°C for 2 min. The thermal cycler was turned off to allow the samples to cool slowly to room temperature. The reaction mixture was placed on ice while adding 2 µl (4 U) *Pfu* DNA polymerase, 2 µl dNTP mix (10 mM each). The reaction mixture was then placed in the block of the cycler at room temperature and the unit was turned on so that the block could slowly heat to 68°C. The reaction mixture was

Table 2. PCR and transformation efficiency comparison between QuickChange site-directed mutagenesis system and our study.

Primer	Molar ratio of mutant products to enterokinase gene products	Molar ratio of mutant products to enterokinase gene products (with cold start)	Transformation efficiency (colonies)
HP_f** /HP_r**	No mutant products could be seen	No mutant products could be seen	0
HP_f* /HP_r*	<1:200	<1:200	3
HP_f /HP_r	<1:200	<1:200	0
HP1_f** /HP1_r**	1: 100	1:100	2
HP1_f* /HP1_r*	1: 30	1:10	200
HP1_f /HP1_r	1: 15	1: 8	30
HP2_f** /HP2_r**	<1:200	<1:200	2
HP2_f* /HP2_r*	1: 100	1: 50	20
HP2_f /HP2_r	1: 50	1: 40	5
EK1_f** /EK1_r**	1: 100	1:100	3
EK1_f* /EK1_r*	1: 20	1:10	300

The single asterisk stands for the primer with the mutation site at the fifth base from the 5'-terminus. The primers without asterisk have the mutation site at the 5'-terminus. The primers which were designed according to the instructions given by Strategene Company were marked with double asterisk.

incubated at this temperature for 5 min followed by 18 cycles of 95℃ for 1 min, 55℃ for 1.5 min, and 68℃ for 14 min. Finally, one cycle of 68℃ was carried out for 14 min in order to evaluate the PCR efficiency. Meanwhile, EK gene (708 bp) was amplified as a control.

At the end of temperature cycling, the PCR products were evaluated by agarose gel electrophoresis. Meanwhile, 10 U (0.5 µl) of *Dpn*I restriction enzymes were added to 8.5 µl PCR reaction mixture and incubated at 37℃ for 1 h. Following *Dpn* I digestion of parental DNA, 5 µl reaction mixture were used to transform XL1-Blue competent cells. The transformed cells were spread onto lysogenic broth (LB) medium plates containing 50 µg/ml kanamycin. A total of 18 colonies (two colonies for each sample, Table 2) were selected and their plasmids were isolated by mini-prep. The positive mutants were verified by sequencing.

Other work preparation

A prerequisite for the success of PCR-based multibase mutagenesis was the development of cost-effective and a generic process for plasmids DNA production. However, to satisfy the strict rule, the material must be available and highly purified with homogeneous super coiled circular covalently closed (ccc) pDNA. Alkaline lyses of the bacteria damages the pDNA, resulting in a reduced recovery of ccc pDNA and an increase in partially open circular forms. Shear stress in these processes needs to be tightly controlled; buffer composition and pH also need to be optimized.

RESULTS AND DISCUSSION

For hexapeptide gene synthesis, we encountered difficulties with the Quick-Change protocol in the course mutational studies, where we were completely unable to introduce any mutation following the recommended protocol (Table 2). These difficulties might be caused by the high self-annealing temperature of primer pair (Table 1), which led to an enormous amount of primer dimers formation and a colossal amount of PCR products reduction.

We developed a simple modification of the primer design, which not only overcame the limitation of self-annealing temperature of primer design, but also made multiple mutations available. The mutant products could be visualized on agarose gel to confirm that the plasmids were successfully amplified. During a 6-base-substitution and a 6-base-deletion-and-1-base-substituion mutagenic PCR, the efficiency was pronounced at a 1:10 molar ratio of mutant products to 705-bp fragment products as control (Table 2) when the mutation was placed as close as five bases away from the 5'-terminus. Typically, around 2.5 µg of asymmetry double-nicked circular DNA was generated from each 50 µl of the PCR reactions. Meanwhile, the transformation efficiency was high (Table 2). The results suggested that the primers in the pair should complement each other at the 5'-terminus instead of the both sides to avoid primer self-extension. Thus, all the self-annealing temperature of inter-primers was not too high.

Comparatively, the amounts of PCR products were more than that earlier described when the mutation was placed at the 5'-terminus but the transformation efficiency is extremely low (Tables 1 and 2). When the mutation was placed at the 5'-terminus, the circularization of PCR products hardly occurred after transformation. Therefore, the transformation efficiency can be used to evaluate the quality of mutant products.

All the 18 multibase mutations were proved correctly through sequencing. In the modification of pET24b-EK, we changed the first five residue of EK, so the N-terminus of the expressed mature recombinant EK would be MVGGS-DSRE. The residue could be cleaved by methionine

aminopeptidase, thereby the modified EK had the same bioactivity as the native EK (Tan et al., 2007). In comparison, all attempts failed if mutant sites started the 5'-terminus in primers or complete overlapping primers were used, even when no products appeared on agarose gel (Table 1 and 2).

A few rules can be deduced from our experiments: (1) The mutation can be placed no less than five bases close to the 5'-terminus and at least 10 to 15 bases from the 3'-terminus; (2) more mutations can be introduced in one primer, with a mutation content up to almost 30% (HP2, 10 out of 38 bases) and (3) cold start PCR appeared to increase the efficiency of PCR (Table 2).

In summary, the methods introduced here was beneficial to broaden the usefulness and facilitate the preparation of high-quality and high-yield MSD, since most reagents were made dead cheaply and no kits were used in the whole process and also documented that, large scale MSD was feasible, efficient, economical, and productive when combined with other methods (Spiess et al., 2010; Zhang et al., 2008).

ACKNOWLEDGMENTS

L. Chen was supported by Grant-in-Aid for JSPS Fellows. This work was partly supported by Grant-in-Aid for Scientific Research (B) from the Ministry of Education, Culture, Sports, Science and Technology (No.21300179) in Japan.

REFERENCES

Falla TJ, Zhang LJ (2010). Efficacy of Hexapeptide-7 on Menopausal Skin. J. Drugs Dermatol. 9: 49-54.

Mullaney EJ, Locovare H, Sethumadhavan K, Boone S, Lei XG, Ullah AH (2010). Site-directed mutagenesis of disulfide bridges in *Aspergillus niger* NRRL 3135 phytase (PhyA), their expression in Pichia pastoris and catalytic characterization. Appl. Microbiol. Biotechnol. 87: 1367-1372.

Shaya D, Zhao WJ, Garron ML, Xiao Z, Cui Q, Zhang Z, Sulea T, Linhardt RJ, Cygler M (2010). Mechanism mechanism of heparinase II investigated by sitesite-directed mutagenesis and the crystal structure with its substrate. J. Biol. Chem. 285: 20051-20061.

Spiess AN, Mueller N, Ivell R (2004). Trehalose is a potent PCR enhancer: Lowering of DNA melting temperature and thermal stabilization of Taq polymerase by the disaccharide trehalose. Clin. Chem. 50: 1256-1259.

Tan H, Wang J, Zhao ZK (2007). Purification and refolding optimization of recombinant bovine enterokinase light chain overexpressed in *Escherichia coli*. Protein Expr. Purif. 56: 40-47.

Zhang ZZ, Shen CC, Wang MC, Han H, Cao XH (2008). Aqueous suspension of carbon nanotubes enhances the specificity of long PCR. Biotechniques, 44: 537-545.

Zhao XB, Suarez J, Khajo A , Yu S, Metlitsky L, Magliozzo RS (2010). A radical on the Met-Tyr-Trp modification required for catalase activity in catalase-peroxidase is established by isotopic Labeling labeling and site-directed mutagenesis. J. Am. Chem. Soc. 132: 8268-8269.

Zheng L, Baumann U, Reymond JL (2004). An efficient one-step site-directed and site-saturation mutagenesis protocol. Nucleic Acids Res. 32: e115.

Int. J. Mol. Sci. **2010**, *11*, 4962-4972; doi:10.3390/ijms11124962

OPEN ACCESS

International Journal of
Molecular Sciences
ISSN 1422-0067
www.mdpi.com/journal/ijms

Article

Optimization of Bacterial Plasmid Transformation Using Nanomaterials Based on the Yoshida Effect

Haidong Tan [1], Li Fu [2] and Masaharu Seno [3,*]

[1] Biotechnology Department, Dalian Institute of Chemical Physics, Chinese Academy of Sciences, Dalian 116023, China; E-Mail: hdt@dicp.ac.cn

[2] Department of Breast Cancer Pathology and Research Laboratory, State Key Laboratory of Breast Cancer Research, Cancer Hospital of Tianjin Medical University, Tianjin 300060, China; E-Mail: fulijyb@hotmail.com

[3] Department of Medical and Bioengineering Science, Graduate School of Natural Science and Technology, Okayama University, Okayama 700-8530, Japan

* Author to whom correspondence should be addressed; E-Mail: mseno@cc.okayama-u.ac.jp.

Received: 21 October 2010; in revised form: 15 November 2010 / Accepted: 1 December 2010 / Published: 3 December 2010

Abstract: With the help of sepiolite, a unique method for transforming DNA into bacteria, based on the Yoshida effect, has been developed recently. However, we confronted many problems when this newest method was tried. Only a few transformants could be obtained even when 100 ng of plasmid pET15b was used, and a successful result seemed difficult to repeat. To address this problem, we optimized the operating method and could achieve about 15,000 transformants using the same amount of plasmid, which could match the efficiency gained using the calcium chloride transformation method. Meanwhile, the results could also be reproduced well. In the same way, carbon nanotubes were used to attain more than 15,000 transformants in the same situation. Therefore, the transformation method could be extended to other nanomaterials. Meanwhile, compared with the mechanism previously reported, we verified quite a different principle for the mechanism responsible for such a transformation. In sum, this unique transformation can be developed to become the third widely-used transformation method in laboratories in addition to the chemical method and electroporation.

Keywords: sepiolite; carbon nanotube; plasmid transformation; nanomaterials; Yoshida effect

1. Introduction

In 2001, Yoshida and colleagues published a novel transformation method based on the inoculation of transforming DNA into bacteria by means of mineral nanofiber [1]. However, little notice has been taken of this very interesting invention because (i) the published work referred to the use of chrysotile asbestos fibers, which had carcinogenic potential and biological activity [2]; and (ii) the authors suggest the usage of a specific apparatus for optimized application of sliding friction forces, which could discourage possible users [3]. In 2010, Wilharm and colleagues improved the method based on the Yoshida effect using another mineral nanofiber (sepiolite) [4], which had been introduced by Yoshida and Sato [5]. Sepiolite—an inexpensive, resourceful, fibrous yet inoffensive mineral—makes DNA transformation rapid and simple. However, we confronted many problems using the novel method: The result seemed difficult to repeat and only a few tranformants could be obtained even when 100 ng of plasmids were used. In this case, we optimized the protocol, but it was difficult to attain more than 3,000 of transformants when 100 ng plasmid pET15b was used.

To address this problem, we changed the operating method and thereby enhanced the transformation efficiency greatly, which could match with that gained from chemical method. We guessed that such a transformation could be extended to other nanomaterials. For example, carbon nanotubes (CNTs) are widely used in most labs and are well characterized [6]. CNTs have been reported as a DNA carrier during the electroporation [7]; however the results cannot point to CNTs making plasmid transformation occur, so the utilization of CNTs for DNA transformation is still unreported. Using our new method, we tried plasmid transformation based on CNTs and got more than 15,000 transformants for 100 ng pET15b.

From these results and combining with those of other experiments, we found that the present mechanism could not explain our findings, so an alternative mechanism was provided here. Meanwhile, with more and more nanomaterials being invented, we hope this unique transformation can be developed to be a third widely-use method in most labs in addition to the chemical method and electroporation.

2. Results and Discussion

2.1. Optimization of Parameters for Plasmid Transformation by Means of Sepiolite

We confronted many problems when we repeated the procedure provided in a previous report [4], and only a few transformants could be obtained although 100 ng of plasmid pET15b was used (Figure 1, sample 6). Moreover, the work was challenging to repeat. Therefore, we optimized various parameters for such a transformation method. We found that the sepiolite buffer was not necessary since the result was no better that when LB medium was used (Figure 1, samples 1 and 2). Furthermore, the cultured cells could be transformed by plasmids in LB medium directly. On the other hand, 0.01% sepiolite was too low to be successful for such a transformation (Figure 1, samples 6–8). Additionally, the time of streaking the plate to spread the transformed cells could affect the efficiency of plasmid transformation greatly (Figure 1, samples 9–12).

Figure 1. The optimization of DNA transformation for *Escherichia coli* DH5α based on sepiolite. (**1–2**) The effect of sepiolite buffer on transformation frequency: Sepiolite buffer was used in sample 1 and LB medium was used directly in sample 2; (**3–5**) The effect of varying cell concentration: $OD_{600\ nm}$ = 200, 20 and 2 in sample 3, 4 and 5 respectively; (**6–8**) The effect of percent content of sepiolite: 1%, 0.1% and 0.01% in sample 6, 7 and 8 respectively; (**9–12**) The effect of time of streaking to plate the transformed cells: 10, 20, 40 and 100 s in sample 9, 10, 11 and 12 respectively; (**13–15**) The effect of washing treatment with ddH_2O on transformation frequency. Sample 13, DNA-binding sepiolite. The DNA-binding sepiolite was washed once and twice by ddH_2O in sample 14 and 15; (**16–18**) The effect of RNA competition on transformation frequency. Sample 16, no RNA was added. For sample 17 and 18, 300 ng and 3 μg small RNA was added in 50 μL transforming solution.

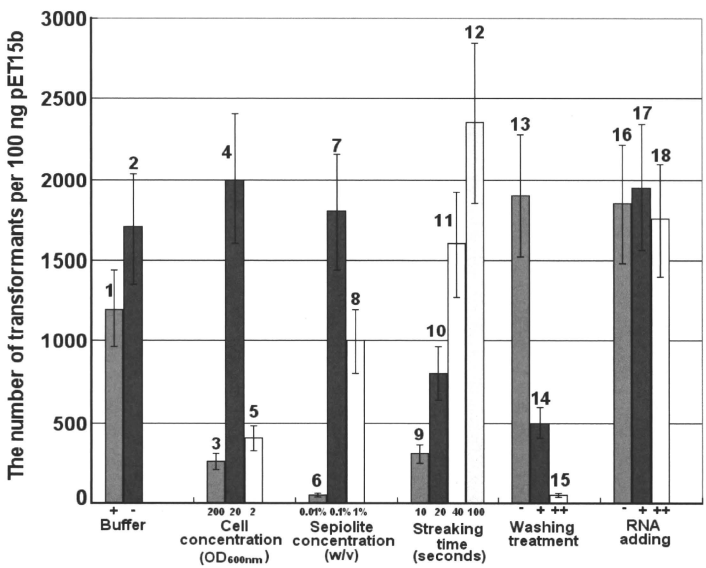

2.2. Plasmid Transformation by Means of Sepiolite and Vortex Operation

Even after the optimization mentioned above, high-efficiency transformation was still difficult to achieve. We decided to repeat the work using a vortex since all parameters could be more easily controlled in a microtube. Thus, we repeated the plasmid transformation with vortexing the mixture (plasmid, sepiolite and cell in LB medium) vigorously in a microtube. Just as we expected, 15,000 transformants per 100 μg of pET15b could be attained, which matched the efficiency obtained from the calcium chloride transformation (8,000 transformants per 100 ng of pET15b) (Figure 2, samples 4–7 and 10). For the operation, one point should be considered carefully. The transformation efficiency was reduced greatly when the volume of the mixture was more than 100 μL in a 500-μL

microtube. We also found the efficiency increased when the vortex time was prolonged. However, the enhancement was slight for vortexing times longer than 5 min although there was no trend for the transformation efficiency reducing with time (Figure 2). Additionally, longer vortex time had no detrimental effect on cell viability or morphology.

Figure 2. DNA transformation for *Escherichia coli* DH5α based on sepiolite and vortex mixing. (**1–3**) Untreated sepiolite (sepiolite 1), the sepiolite collected from the supernatants (sepiolite 2) and ultrasonicated sepiolite (sepiolite 3); (**4–7**) Effect of varying vortex operation time for sepiolite 1, from 1 to 10 min; (**8–9**) Untreated CNTs (CNTs1) and ultrasonicated CNTs (CNTs2). $CaCl_2$ refers to chemical transformation method.

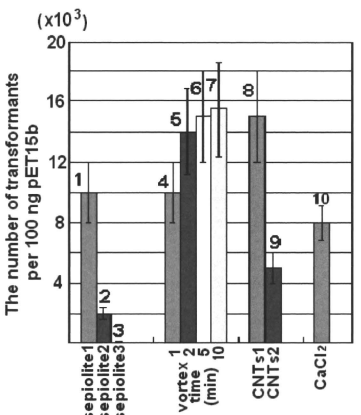

2.3. Plasmid Transformation by Means of CNTs

Since the plasmid transformation performed well using nanofibers, the method should be extended to other nanomaterials. For this purpose, we used CNTs in the transformation and obtained more than 15,000 transformants per 100 ng pET15b, which was more than we obtained using a traditional chemical method (Figure 2, samples 8 and 10). However, the result could not be explained by the fibers causing piercing of the bacterial cell wall, because we observed that many CNTs were congregated together under the microscope while the ultrasonicated CNTs failed to produce more transformants (Figure 2, sample 9). To identify an alternative explanation for the mechanism of the transformation, the work described below was performed.

2.4. Mechanism for the Plasmid Transformation by Means of Nanomaterials

Previously, the mechanism for the transformation method based on the inoculation of transforming DNA into bacteria by means of mineral nanofiber was explained as follows: When a colloidal solution containing mineral nanofibers is mixed with bacteria and transforming DNA and plated on selective agar plates, the sliding friction forces, arising between the surface of the agar and the stir stick when

bacteria are spread, result in penetration of bacterial cells, which leads to inoculation of the transforming DNA that is adsorbed to the mineral nanofibers. Inside the cell, the DNA is probably displaced by competition with small nucleic acids [4], so that it can be maintained and expressed. According to this mechanism, it was obvious that the transformation efficiency would be reduced greatly if enough small RNA was added to the mixture because this transformation with exogenous DNA was closely related to the phenomenon based on the Yoshida effect. To test the hypothesis, the following experiments were prepared.

Firstly, as shown in Figure 3, lane 5, high-quality 300-bp RNA (300 ng/μL) was extracted from *Lactobacillus brevis* AS1.579 and prepared according to the method described in a previous report [8], and briefly in the Experimental Section. Through a competitive absorbtion test, we found that the DNA on the sepiolite could not be replaced by 300 ng/μL RNA (Figure 3, lane 6). The DNA could not even be eluted out by 5 M NaCl (data not show), but could be eluted out by 400 mM guanidine hydrochloride, pH 4.0 (Figure 3, lane 7). This result indicated that the DNA absorbed sepiolite tightly and could not be displaced by RNA. On the other hand, washing treatment with ddH_2O could affect plasmid transformation greatly (Figure 1, samples 13–15). All together, these results implied that it was unlikely that the mechanism for the plasmid transformation was mainly caused by sepiolite carrying the DNA into cells and being displaced by RNA. The number of the transformants was mainly determined by the amount of DNA in the solution but not determined by the amount of the DNA bound on the sepiolite.

To further investigate this, we performed the following experiment. The sepiolite was absorbed to saturation with the RNA (after centrifugation, the $OD_{260\,nm}$ value of the supernatant was not reduced any more for 0.1% sepiolite solution (w/v) when more than 6 ng/μL final concentration RNA was added) and then mixed with suitable amounts of the plasmids. The result indicated the small RNA did not affect the DNA transforming frequency compared to the sample without RNA addition (Figure 1, samples 16–18). Thus, small RNA did not inhibit the DNA transformation frequency; namely, the DNA absorbed on the nanofibers would not be displaced by competition with small nucleic acids in the cell [4].

Additionally, we selected two other sepiolites (sepiolite 2 and 3) with more fibers compared with sepiolite 1 (the untreated sepiolite), see Figure 4. Sepiolite 2 is the sepiolite collected from the supernatants and sepiolite 3 is ultrasonicated sepiolite (Figure 4). According to the mechanism supplied by previous reports [4], sepiolite with more nanofibers will produce higher-efficiency transformation. Conversely, the transformation efficiency was reduced greatly, and even failed to produce transformants when ultrasonicated sepiolite was used, while the transformation efficiency was the highest when the sepiolite was untreated (Figure 2, samples 1–3). In the same way, using CNTs produced similar results. These results suggested that the fibers alone hardly influenced the success of the plasmid transformation. Heterogeneous DNA still could enter the cell even without absorbing on the sepiolite fibers. The transformation might need the larger size of sepiolite to destroy the cell wall for the plasmids to enter the cell envelope through the temporary nanochannels formed in the cell membrane.

Figure 3. 1% agarose analysis of DNA-binding after sepiolite washing and competitive absorbtion with small RNA. **Lane 1**: pET15b expression vector (~5.3 Kb); **Lane 2**: DNA binding sepiolite to saturation; **Lane 3**: DNA binding sepiolite to saturation was washed once with water; **Lane 4**: DNA binding sepiolite to saturation was washed with water twice; **Lane 5**: Small RNA (~300 bp) extracted from *Lactobacillus brevis* AS1.579; **Lane 6**: The mixture of DNA-binding sepiolite and small RNA; **Lane 7**: DNA-binding sepiolite was eluted by 400 mM guanidine hydrochloride, pH 4.0. Note: After electrophoresis, the DNA stayed at the sample loading position due to the strong absorbing power between the DNA and sepiolite (**Lanes 2–4, 6**).

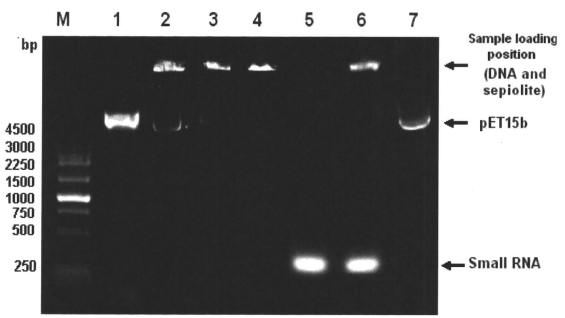

Figure 4. After absorbing GFPuv, the shape of sepiolite is observed by fluorescence microscope. There are three kinds of sepiolite: untreated sepiolite (sepiolite 1), the sepiolite collected from the supernatants (sepiolite 2) and ultrasonicated sepiolite (sepiolite 3).

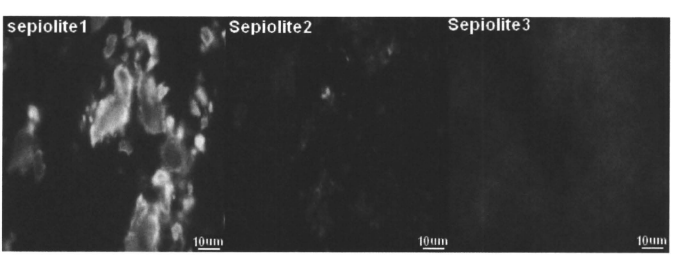

The most widely used methods for DNA transformation of eukaryotes are chemical transformation and electroporation. However, both methods require preparation of competent cells and recovery, which are time-consuming and tedious. Furthermore, existing electroporation technology is limited in its ability to treat large quantities of cells and DNA. Additionally, the application of an expensive electroporation apparatus and a specialized power supply can lead to irreversible electroporation and, consequently, cell lysis [9]. In some routine experiments, high efficiency is as important as time and convenience. Thus, in 2001, Yoshida and colleagues published many exciting papers describing a novel transformation method based on mineral nanofibers [10–13]. In 2010, Wilharm *et al.* further improved the method [4].

However, we found that this latest technology still needed optimization to be widely used in most labs because we obtained low-efficiency transformation. Therefore, we optimized the protocol and changed the operation. Following our optimization, high-efficiency transformation could be reached and the results could be repeated well. In addition, through our work, we found that the present mechanism proposed to explain the transformation could not explain our results. From our results, we propose that the mechanism for the DNA transformation based on sepiolite might be explained as follows: the formation of nanochannels is driven by nanomaterials through the bouncing forces arising among the nanomaterials, bacteria and microtubes during the vortex mixing step. The heterogeneous DNA can simultaneously enter the cells via the nanopores, so that it can be maintained and expressed. To produce enough bouncing forces, the nanofibers should be fixed on the large particles of the nanomaterial aggregates (Figure 5d). Otherwise, only nano-size fibers failed to produce transformants (Figure 4 and Figure 2, sample 3).

Figure 5. The hypothesis for the mechanism of plasmid transformation by means of nanomaterials. (**a**–**c**) The model for the process of heterogeneous DNA entering a cell with the help of nanomaterials; (**d**) the cartoon structure of nanofiber and nanomaterial aggregates.

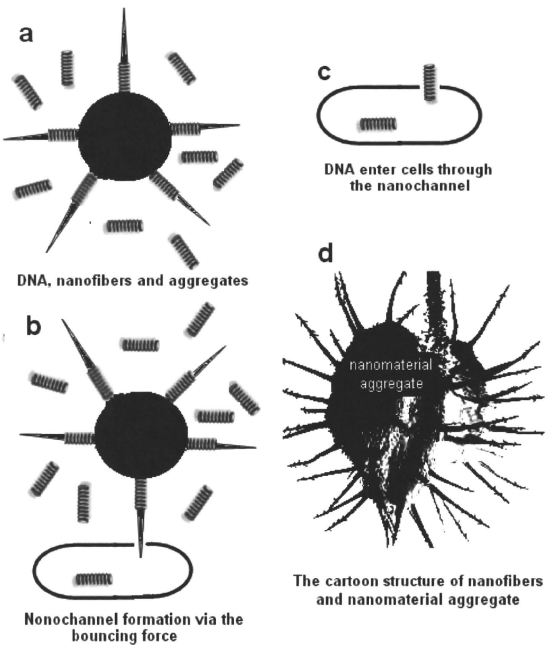

In any way, based on nanomaterials, the transformation offer several advantages over the chemical method and electroporation: (1) The experiment can be performed conveniently at any time. For

instance, DNA transformation will occur just by shaking when the sepiolite is mixed with heterogeneous DNA and bacteria in a microtube; (2) small amount of cells can be transformed by plasmids easily. For example, a single colony can be transformed by plasmids directly even when the colony has been stored on a plate at 4 °C for more than one month; (3) the experiment for the reception of some pathogens to various plasmids can be performed easily based on nanomaterials; (4) with the help of the plasmid pKD46, linear DNA can be transferred into bacteria; work which always fails via the chemical method. With more invent of nanomaterials, there are still many possibilities for the development of the transformation method. This method should be developed to become a third widely-used method in addition to the electroporation and chemical transformation methods.

On the other hand, the following work is needed to be done in the future. The method is never used for eukaryote transformation and special species. For example, electroporation and the chemical transformation method seem to be difficult to use in the areas where cell surfaces are hard, such as Gram positive bacteria or plant cells. In these cases, the plasmid transformation by means of nanomaterials may be a good choice.

3. Experimental Section

3.1. Materials and Strains

Plasmid pET15b was purchased from Novagen (Merck KGaA, Darmstadt, Germany). *Escherichia coli* DH5α, cell culture components, guanidine thiocyanate, phenol, proteinase K and plasmid minipreparation kits were supplied by Dingguo Biotech (Beijing, China). *Lactobacillus brevis* AS1.579 was obtained from The Institute of Microbiology, Chinese Academy of Sciences (Beijing, China). Sepiolite was purchased from Kremer Pigmente GmbH & Co. KG (Hauptstr, Aichstetten, Germany). Carbon nanotube (95%, 8–15 nm) was purchased from TimesNano (Chengdu, China). Recombinant green fluorescent protein (GFPuv) was expressed from *Escherichia coli* BL21 and purified in our lab.

3.2. Cell Culture

Escherichia coli DH5α was streaked and grown at 37 °C on Luria-Bertani (LB) plates (10 g/L tryptone, 5 g/L yeast extract, 10 g/L sodium chloride and 1.5% agarose, pH 7.0) for 20 h. One colony from the plate was transferred into 5 mL of LB medium, incubated at 37 °C, 200 rpm for 12 h. The pre-culture was diluted 100-fold to inoculate 500 mL into LB medium. The culture was allowed to grow with shaking (200 rpm) at 37 °C until the $OD_{600\,nm}$ reached 0.4. The cells were collected via centrifugation at 4 °C for 10 min at 3,000 × g. All the precipitation was resuspended in 1 mL sepiolite buffer, and stored on ice for the next step.

3.3. Optimization of Parameters for Plasmid Transformation by Means of Sepiolite

The following parameters were optimized: sepiolite buffer, cell concentration, sepiolite concentration, and the length of time spent streaking the cells on plates after transformation (Figure 1). Sepiolite buffer was prepared as previous reported [4]. One hundred microliters of transforming mixture consisting of 0.1% sepiolite (w/v), bacteria ($OD_{600\,nm}$ = 20) and 100 ng pET15b were spread

on a 2% agar plate with 100 μg/mL ampicillin unless otherwise indicated. The suspension was spread with polystyrene or glass stir sticks until the liquid was completely soaked into the agar, which is indicated by a marked increase of frictional resistance, and spreading was then continued for an additional 30 s unless otherwise indicated. Plates were incubated at 37 °C overnight.

3.4. Plasmid Transformation by Means of Sepiolite and Vortex Operation

Fifty microliters of transforming mixture consisting of LB, bacteria ($OD_{600\ nm}$ = 20), 0.1% sepiolite and 100 ng of DNA were transferred into a 500-μL microtube. The mixture was subjected to a vortex mixer (Vortex-Genie 2, Model G560E; Scientific Industries, Inc. Bohemia, New York, USA) at full speed for 1, 2, 5 or 10 min. The vortexed cells were spread on a 1.5% agar plate with 100 μg/mL ampicillin and incubated at 37 °C overnight.

3.5. Plasmid Transformation by Means of CNTs

Fifty microliters of transforming mixture consisting of LB, bacteria ($OD_{600\ nm}$ = 20), 0.1% CNTs and 100 ng pET15b was transferred into a 500-μL microtube. The mixture was subjected to a vortex mixer at full speed for 1 min. The cells were then spread on a 1% agar plate with selective antibiotics (100 μg/mL ampicillin) and incubated at 37 °C overnight.

3.6. Plasmid Transformation by the Calcium Chloride Method

Escherichia coli cells were made competent for plasmid transformation by the calcium chloride method [14]. One hundred microliters of competent cells were taken and 100 ng pET15b were added. The mixture was incubated on ice for 30 min and then heat shocked at 42 °C for 90 s. The transformation mixture was incubated on ice for 2 min. Four hundred microliters of LB medium was added and the mixture incubated at 37 °C for 45 min in an incubator-shaker. Fifty microliters of the mixture was spread onto a LB plate with ampicillin and incubated at 37 °C overnight.

3.7. Mechanism for the Plasmid Transformation by Means of Nanomaterials

Theoretically, the DNA bound with sepiolite will not be eluted by ddH_2O because of the strong binding force between the negative charges of DNA and a positive charge cluster of sepiolite. Thus, the amount of DNA in the solution of sepiolite will not affect the number of transformants according to the mechanism supplied by Wilharm [4]. To prove this, we removed the DNA in the solution of sepiolite via washing treatment. One hundred microliters of 0.1% sepiolite suspension (w/v) was mixed with 100 ng pET15b and then centrifuged at 5,000 × g for 2 min. The precipitate was resuspended in 500 μL ddH_2O and the above steps were repeated twice. Finally, the precipitation of sepiolite was resuspended in 90 μL ddH_2O and mixed with 10 μL cells ($OD_{600\ nm}$ = 200) in a 500-μL microtube. The mixture was mixed in a vortex mixer at full speed for 1 min. After mixing in a vortex, the cells were spread on a 1% agar plate with 100 μg/mL ampicillin and incubated at 37 °C overnight.

Small RNA (~300 bp) was prepared from 10 mL late-exponential-phase *Lactobacillus brevis* AS1.579 using the CTAB preparative protocol for bacterial genomic DNA isolation, as described previously with some modification [8] and no RNAase was added. To culture *Lactobacillus brevis*